Int. J. Solids Structures Vol. 24, No. 1, pp. 89–104, 1988
Printed in Great Britain.

0020-7683/88 $3.00 + .00

STIFFENED PLATES SUBJECT TO TRANSVERSE LOADING

J. C. Boot and D. B. Moore
School of Civil Engineering, University of Bradford, Bradford BD7 1DP, U.K.

(*Received* 8 *June* 1987)

Abstract—The generalized conditions under which stiffened plates can be approximated as a two-dimensional continuum are investigated and identified. A simplified set of constitutive equations defining the full class of problems described above, subject to elastic behaviour, are then obtained by making suitable assumptions. The significance of these assumptions is investigated under a wide range of conditions, and the results calculated for typical problems using the simple theory compared with experimentally obtained values. The simple theory is then amended to allow consistently for the effects due to Poisson's ratio in the stiffeners. A study of the resulting equations indicates that whilst the normal assumption of centroidal neutral axes is justified under all conditions, the additional strain energy generated in the stiffeners can be significant, and that under the assumption of centroidal neutral axes this is readily included in the formulation without penalty. Shear effects other than those due to St. Venant torsion are not considered in the detailed analysis.

1. INTRODUCTION

The eccentrically stiffened plate subject to transverse loading is an extremely common structural form. A full three-dimensional analysis of these members is usually avoided by adopting a thin[1] or moderately thick[2] plate theory based on the concept of smoothed flexural, torsional, and transverse shear rigidities. However, the approximation of one structural form by another is an expedient which inevitably raises questions of validity; in the present context, depending on the spacings, sizes, shapes, and orientations of the stiffeners, some or all of the following considerations may merit special attention.

(1) The combinations of stiffener orientations for which the strain distribution throughout the thickness of the structure can be generalized.

(2) The possibility of distortions of the cross-sections.

(3) The laws governing the choice of flexural and torsional properties of the "equivalent" unstiffened plate.

(4) The interaction of the longitudinal direct and shear stresses in the plate (shear lag).

(5) The significance of the transverse shear stresses.

Factors (1) and (2) govern the viability of a 2-D approximation to the problem; assuming these considerations elicit a positive response, then provided the stiffeners are closely spaced (i.e. (4) insignificant), and the plan dimensions are large in comparison to those associated with depth (rendering (5) a minor effect), then attention usually concentrates on the parameters identified in (3), assuming the material properties permit the "equivalent plate" to be defined[3, 4].

The majority of authors considering these problems concentrate on the particular case of a regular shape in plan (usually rectangular) stiffened by a rectangular grid such that an equivalent orthotropic plate, for which there is a known solution, can be identified. Troitsky[5] summarizes the literature in this regard. In this paper we obtain an analysis which is restricted only by the generalized conditions under which the rigidity smoothing process is valid; this implies the following initial assumptions.

(a) The properties of the plate and stiffener vary gradually, and in such a manner that the mid-surface of the plate can be considered as a flat plane with the components of direct stress perpendicular to this plane being everywhere zero.

(b) The geometry of the stiffeners is such that their behaviour can be described by the generalized beam theory[6].

In order to simplify the central arguments without unduly compromising the range of application of the resulting equations, the following further (i.e. non-essential) assumptions are adopted for the purposes of the present study.

(c) The shear centre and centroid of the stiffeners are coincident (transverse shear and torsional stresses independent).

(d) Warping stresses are negligible; i.e. the torsional moments and especially their gradients are not large, and the geometry of the structure (see also (f) below) is not conducive[7] to the generation of significant restrained warping under other loading conditions.

(e) The plate mid-surface is parallel to one principal axis of each stiffener cross-section; stiffeners of variable cross-section must satisfy (a) above[8].

(f) The stiffened plate section will not distort, and the torsional shear stresses in the stiffeners and plate form independent systems (stiffeners form an open cross-section *with* the plate[5], and the width of the stiffeners is not large in comparison to the depth of the plate).

Subject to these restrictions Section 2 investigates the conditions identified under (1) for which a 2-D analysis, assuming only the stress resultants considered in classical thin plate theory are active, is possible. Section 3 develops and tests the resulting generalized theory. The analysis is cast in variational form, thus enabling primary and secondary sources of energy in both plate and stiffeners to be considered independently and the results summed algebraically to describe the overall behaviour. Initially, therefore we further simplify the analysis by making two additional assumptions.

(g) Certain inconsistencies in the treatment of the strains due to Poisson's ratio do not significantly affect the results.

(h) Shear lag and transverse shear effects can be ignored.

In Sections 4 and 5 we investigate the significance of assumption (g) which embraces approximations on the position of the unstrained "surface", and the strain energy stored at the stiffener intersections. These effects have been considered by Cusens *et al.*[9]; however, in the present paper we study them separately rather than concurrently, thus enabling the circumstances under which each may be significant to be identified. Furthermore, the smoothing processes adopted here satisfy the more generalized conditions considered throughout this paper, and obey the Reciprocal Theorem[3] precisely.

In Section 6 we consider briefly how the effects isolated under (h) can be included in the formulation. However, throughout the detailed analysis, all shear effects other than those associated with St. Venant torsion are omitted.

2. THE LIMITATIONS GOVERNING THE APPLICATION OF BENDING AND TORSIONAL RIGIDITY SMOOTHING PROCESSES

Morley[10] has studied the problem of an isotropic plate subject to plane stress conditions and stiffened by arbitrarily oriented sets of parallel (eccentric) stiffeners. He concludes that any anisotropic material subject to plane stress conditions can be modelled as a plate strengthened by up to six sets of such stiffeners.

However, consider an isotropic plate of constant thickness stiffened by two sets of arbitrarily oriented sets of parallel stiffeners and subject to a combination of pure (i.e. constant) bending and twist as illustrated in Fig. 1. Then for equilibrium

$$M_\eta = M_x \sin^2\theta - 2M_{xy}\sin\theta\cos\theta + M_y\cos^2\theta \tag{1}$$

$$M_{\eta\xi} = \sin\theta\cos\theta(M_x - M_y) + M_{xy}(\sin^2\theta - \cos^2\theta). \tag{2}$$

Let us take for simplicity

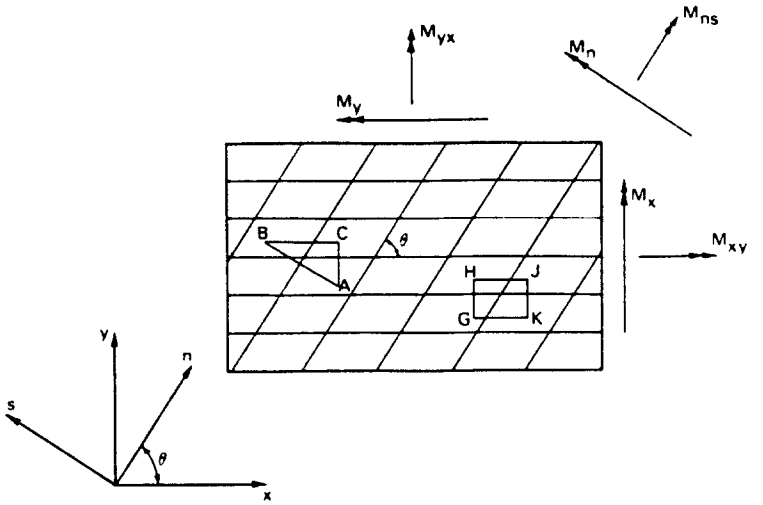

Fig. 1. Plate subject to arbitrary pure bending and strengthened by two randomly oriented sets of parallel stiffeners.

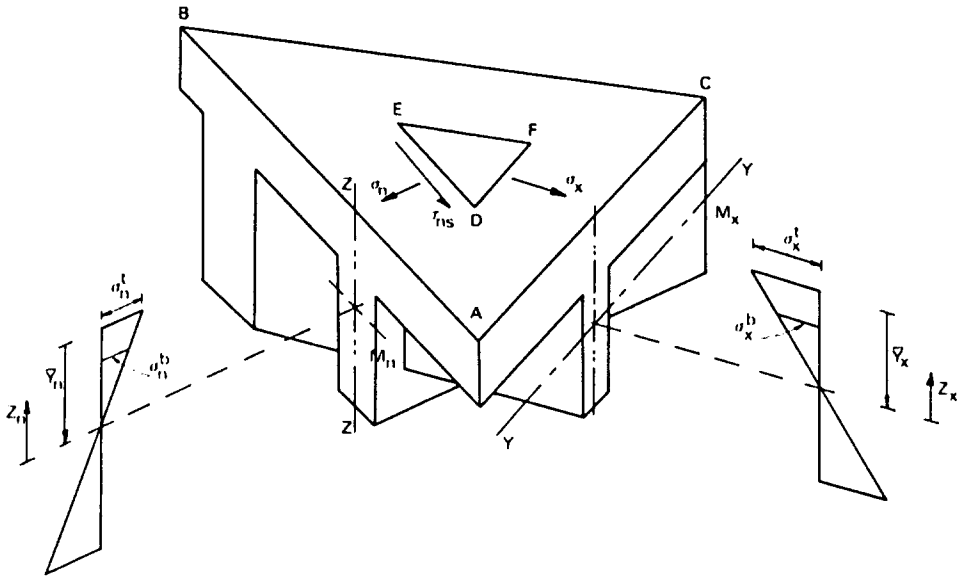

Fig. 2. Consideration of the equilibrium conditions on element ABC taken from the plate delineated in Fig. 1.

$$M_y = M_{xy} = 0. \tag{3}$$

Then whatever the actual stress distribution throughout the plate we must have

$$M_x = \int_{A_x} \sigma_x z_x \, dA_x; \quad M_n = \int_{A_n} \sigma_n z_n \, dA_n \tag{4}$$

$$\int_{A_x} \sigma_x \, dA_x = 0; \quad \int_{A_n} \sigma_n \, dA_n = 0 \tag{5}$$

$$\sigma_z = 0 \text{ everywhere}; \quad \tau_{xz} = \tau_{yz} = \tau_{xy} = 0 \text{ on all boundaries} \tag{6}$$

where the terminology is defined in Fig. 2.

Now under the generalized conditions being considered throughout this paper, and defined in Section 1, the following arguments govern the validity of any smoothing process.

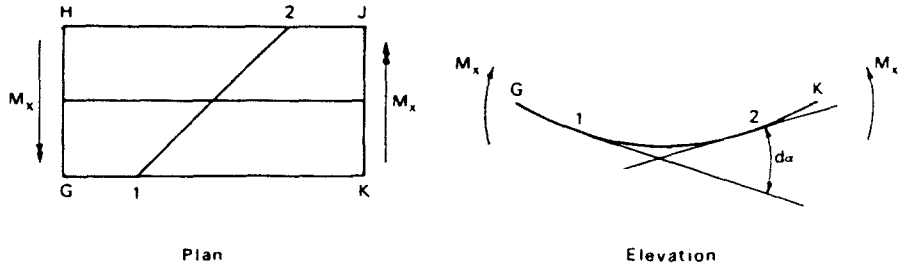

Fig. 3. Details of the deformation of element GHJK taken from the plate of Fig. 1.

(a) The proportion of the total area of the problem over which the properties are smoothed must be small enough to approximate to an element subject to constant bending and twist such as that shown in Fig. 1.

(b) The smoothing process must yield a unique solution for equilibrium in the original plate when subject to constant M_x, M_y, M_{xy}.

(c) The acceptance of a weighted average solution to eqns (1)–(4) permits[11] arbitrary movements of the depth of the neutral axis[12] which in turn permits arbitrary violations of eqn (5). Thus bending rigidities so derived in general contain unbounded errors, and we surmise therefore that the adopted smoothing process must provide an exact solution to (b) above. This is equivalent to requiring that the solution process satisfy the patch test[2].

Consider therefore the behaviour of element ABC taken from the plate of Fig. 1. Figure 2 shows the usual linear distribution of bending stresses throughout the full depth of the stiffened plate, but the results are qualitatively unaffected if any generalized assumption satisfying eqns (4) and (5) is substituted. Let us assume therefore that the bending stress distributions illustrated in Fig. 2 pertain; then since the direct stresses at any depth are constant it follows from eqn (6) that τ_{xz}, τ_{yz} are everywhere zero. It now follows that the horizontal stresses σ_x, σ_n, τ_{xn} at any point in the plate (see e.g. point DEF in Fig. 2) must form a system in equilibrium over any elemental depth dz, whence

$$\sigma_n^i = \sigma_x^i \cos^2 \theta \tag{7}$$

applying eqn (7) at i = t, b (see Fig. 2) yields

$$\bar{\gamma}_n = \bar{\gamma}_x, \quad \text{i.e.} \quad \bar{\gamma}_n = f(\bar{\gamma}_x) \quad \text{for} \quad \theta \neq 90^\circ . \tag{8}$$

However, since $\bar{\gamma}_n$ is a function of the dimensions of the stiffeners in the n-direction and $\bar{\gamma}_x$ is not, it is clear that in general

$$\bar{\gamma}_n \neq f(\bar{\gamma}_x) \quad \text{for all} \quad \theta. \tag{9}$$

Equations (8) and (9) are only compatible for $\theta = 90^\circ$, i.e. the bending stress distributions illustrated in Fig. 2 can only exist in orthogonally reinforced plates. The reason for this is evident from a study of the element GHJK taken from the plate of Fig. 1. Figure 3 shows that the ends of the stiffeners 1–2 are twisted through an angle $d\alpha$ which is only zero when $\theta = 0^\circ$ or 90°; the stresses associated with this deformation have been excluded from the analysis above.

The more complex treatment required to take the above deformations into account must inevitably link $w_{,xx}$ $w_{,yy}$ and the twisting moments, whilst simplified methods for assessing twisting rigidities are independent of M_x and M_y. Furthermore, the twist generated on the element shown in Fig. 3 has opposite effects on faces HG, JK. Thus when two adjacent such elements are bent together, if the faces to which the bending moments M_x are applied are not to twist (i.e. satisfy the displacement boundary conditions for pure bending), compatibility at the common interface must induce a rippling of the plate which

in general destroys the concept of an element of a stiffened plate subject to constant curvature conditions.

It would seem therefore that a 2-D approximation can only be theoretically justified if the stiffeners form a random orthogonal network with the material properties everywhere defined by planes of material symmetry[3, 4] coincident with the stiffener orientations, due to the difficulty in obtaining 2-D constitutive equations which satisfy either Betti's law[3] or requirements (b) and (c) above in more generalized situations. The practical examples of this class of problem include plates of arbitrary plan shape reinforced in a rectangular, fan, or isostatic[5] manner.

3. VARIATIONAL FORMULATION OF THE SMOOTHING PROCESS

The generalized variational principle in elasticity can be written as[13, 14]

$$\delta[U(\varepsilon_{ij}) + D_1(\varepsilon_{ij}, \sigma_{kl}) + P_1(u_i)] = 0 \tag{10}$$

or

$$\delta[W(\sigma_{ij}) + D_2(\sigma_{ij}, \varepsilon_{kl}) + P_2(\sigma_{ij})] = 0 \tag{11}$$

where U, W are the strain and complementary energies in the system, respectively, D_1 the function of independently defined strains and stresses removing the requirement that the strains satisfy the compatibility equations, D_2 the function of independently defined stresses and strains removing the requirement that the stresses satisfy the equilibrium equations, and P_1, P_2 the work done by the applied loading and prescribed displacements, respectively.

In eqns (10) and (11) all displacements (u_i), strains (ε_{ij}), and stresses (σ_{ij}) can be approximated independently, whence weighted average solutions for equilibrium and compatibility are obtained provided the constitutive equations can be specified. Equations (10) and (11) are derivable from one another, and all other variational forms can be obtained from whichever is more convenient and applying the appropriate constraints to the field variables. Now as only U and W are functions of the constitutive equations it is clear that in the present context, provided we can ensure equivalence of both U and W between the actual and smoothed problems over an elemental area of the plate, then a solution can be obtained (provided suitable approximating functions can be found).

For the class of problem under consideration U and W are normally expressed[1] as

$$U = \frac{1}{2}\int_V (\sigma_{xx}\varepsilon_{xx} + \tau_{xy}\gamma_{xy} + \sigma_{yy}\varepsilon_{yy})\,\mathrm{d}V = \int_V \Omega(\varepsilon_{ij})\,\mathrm{d}V \tag{12}$$

$$W = \frac{1}{2}\int_V (\sigma_{xx}\varepsilon_{xx} + \tau_{xy}\gamma_{xy} + \sigma_{yy}\varepsilon_{yy})\,\mathrm{d}V = \int_V \varphi(\sigma_{ij})\,\mathrm{d}V \tag{13}$$

where Ω and φ are the strain and complementary energy densities. Furthermore, for linear elasticity, from Clapyron's theorem[3] $U = W$ whence

$$\{\sigma\} = [D]\{\varepsilon\}; \quad \{\varepsilon\} = [C]\{\sigma\}; \quad [D] = [C]^{-1} \tag{14}$$

and thus attention can be focused on U or W, whichever is more convenient.

For plastic (and non-linear elastic) applications eqns (10)–(13) must be written in incremental form and the constitutive equations may not possess a unique inverse; nevertheless the problem can be linearized over an appropriately small increment of load and δU, δW evaluated[13, 15]. However, limiting attention to linear elastic orthotropic behaviour for simplicity, we have[4] for the non-zero elements of $[D]$

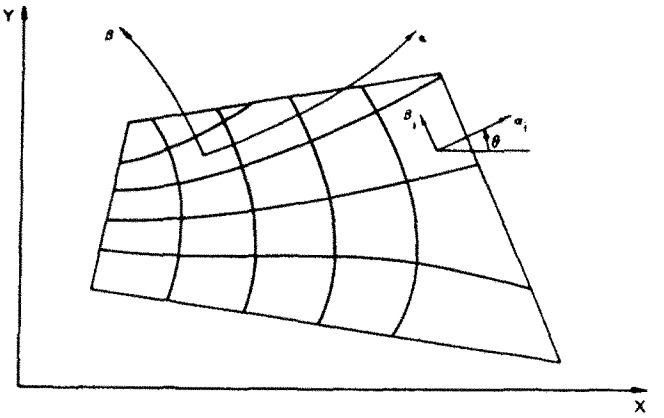

Fig. 4. Arbitrary orthogonally stiffened plate with the directions of the stiffeners everywhere coincident with the curvilinear coordinates α, β.

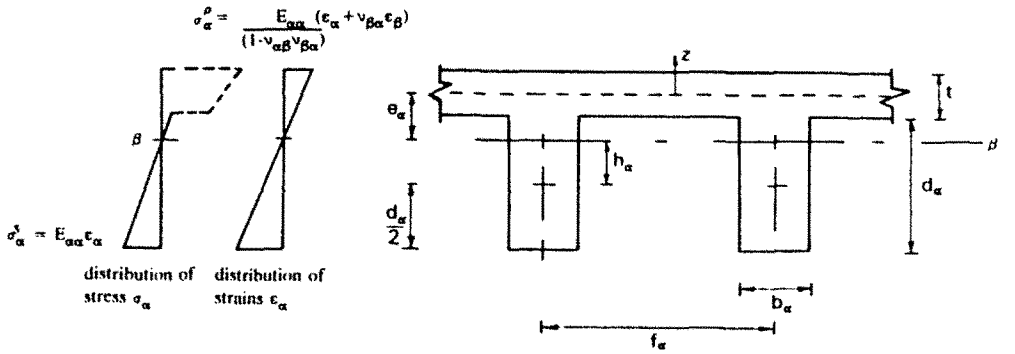

Fig. 5. Section β β through the plate of Fig. 4 showing dimensions and basic assumptions concerning the strain and stress distribution in the α-direction.

$$D_{11} = \frac{E_{xx}}{1-\nu_{x\beta}\nu_{\beta x}}; \quad D_{12} = D_{21} = \frac{E_{\beta\beta}\nu_{x\beta}}{1-\nu_{x\beta}\nu_{\beta x}}; \quad D_{22} = \frac{E_{\beta\beta}}{1-\nu_{x\beta}\nu_{\beta x}}; \quad D_{33} = G_{x\beta}. \tag{15}$$

Equations (14) and (15) relate the components of stress and strain defined in a system of curvilinear coordinates (α, β) in the plane of the plate which are everywhere coincident with the directions of geometric and material orthogonality (see Fig. 4). Then taking into account eqns (4), since energy is a scalar quantity we can write the strain energy density in the stiffened plate as

$$\Omega_i (= \varphi_i) = \Omega_i^p + \Omega_i^x + \Omega_i^\beta \tag{16}$$

where

$$\Omega_i^p = \tfrac{1}{2} M_{x\beta} w_{,x\beta}$$
$$= \text{strain energy/unit area of plate at point } i \tag{17}$$

$$\Omega_i^x = \Omega_i^x, \quad \Omega_i^\beta = \tfrac{1}{2}[M_{ss}^x w_{ss}^x + M_{ns}^x w_{ns}^x]$$
$$= \text{strain energy/unit area of plate in each set of stiffeners at point } i \tag{18}$$

where M_{ss}, M_{ns} are the bending and torsional moments in a stiffener per unit area of plate.

In order to simplify the solution, we now make α, β coincide with the appropriate neutral axes of the whole section at point i. Then from Figs 5 and 6 and Refs [1, 5, 10] (note also the experimental evidence in support of the assumption of independent shear stress systems in the plate and stiffeners given in Ref. [9]), the strains and moments of the stresses in the plate about the neutral axes at the point are given by

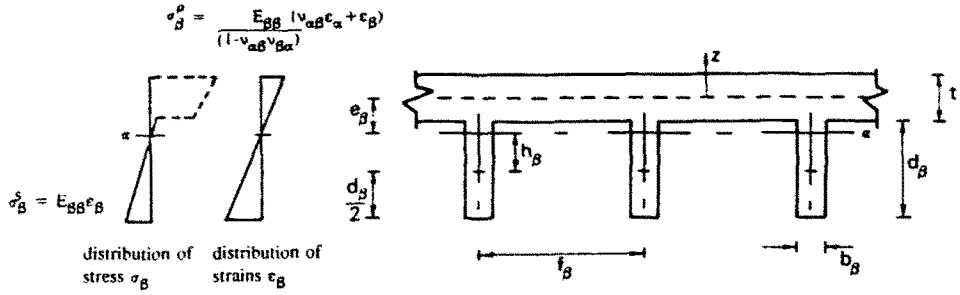

Fig. 6. Section x x through the plate of Fig. 4 showing dimensions and basic assumptions concerning the strain and stress distribution in the β-direction.

$$\left.\begin{aligned}
\varepsilon_x &= (z+e_x)w_{,xx}; \quad M^{\mathrm{p}}_{xx} = \int_{-t/2}^{t/2} (D_{11}\varepsilon_x + D_{12}\varepsilon_\beta)(z+e_x)\,\mathrm{d}z \\
\varepsilon_\beta &= (z+e_\beta)w_{,\beta\beta}; \quad M^{\mathrm{p}}_{\beta\beta} = \int_{-t/2}^{t/2} (D_{12}\varepsilon_x + D_{22}\varepsilon_\beta)(z+e_\beta)\,\mathrm{d}z \\
\gamma_{x\beta} &= 2w_{,x\beta}; \quad M^{\mathrm{p}}_{x\beta} = \int_{-t/2}^{t/2} D_{33}\gamma_{x\beta} z\,\mathrm{d}z
\end{aligned}\right\} \tag{19}$$

and in the stiffeners ($j = x, \beta$)

$$M^j_{xx} = \frac{D_{11}b_j}{f_j}\int_{(t/2+d_j)}^{t/2} \varepsilon_j z\,\mathrm{d}z; \quad M^j_{xs} = \frac{G_{x\beta}}{f_j} T_j d_j w_{,x\beta} \tag{20}$$

where T_j is as defined in Ref. [12].

Substituting eqns (17)–(20) into eqn (16) yields

$$\Omega_i = \tfrac{1}{2}\{w_{,x\beta}\}_i^t [D']\{w_{,x\beta}\}_i \tag{21}$$

where

$$\{w_{,x\beta}\}_i^t = \{w_{,xx}\ w_{,\beta\beta}\ w_{,x\beta}\}_i \quad \text{at point } i$$

$$[D'] = [D'_{x\beta} + D'_{x0} + D'_{0\beta}]$$

$$D'_{x\beta} = t\begin{bmatrix} D_{11}\left(\dfrac{t^2}{12}+e_x^2\right) & D_{12}\left(\dfrac{t^2}{12}+e_x e_\beta\right) & 0 \\ D_{12}\left(\dfrac{t^2}{12}+e_x e_\beta\right) & D_{22}\left(\dfrac{t^2}{12}+e_\beta^2\right) & 0 \\ 0 & 0 & D_{33}\dfrac{t^2}{6} \end{bmatrix};$$

$$D'_{x0} = \frac{1}{f_x}\begin{bmatrix} E_{xx}\left(\dfrac{b_x d_x^3}{12} + b_x d_x h_x^2\right) & 0 & 0 \\ 0 & 0 & 0 \\ 0 & 0 & D_{33}T_x \end{bmatrix}$$

define the contributions of the plate and stiffeners in the x-direction, respectively. $D'_{0\beta}$ can be deduced by permutation, and the prime is a reminder that the (smoothed with respect to depth) obtained values are not necessarily moment curvature relationships[11], the

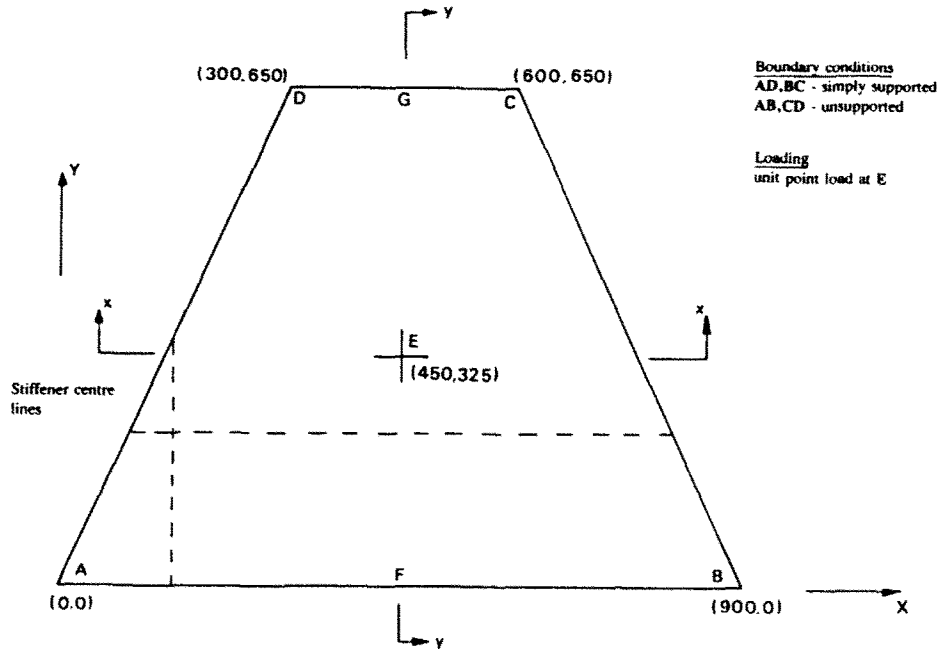

Fig. 7. Plan dimensions and boundary conditions of the trapezoidal plate ABCD considered in Section 3. All dimensions in mm.

stresses in the plate and stiffeners are related to the curvatures through eqns (19), (14), and (15).

Now $\{w_{,\alpha\beta}\}$ transforms as a second-order Cartesian tensor[16], i.e.

$$\{w_{,\alpha\beta}\} = [\lambda]\{w_{,xy}\} \tag{22}$$

where

$$[\lambda] = \begin{bmatrix} \cos^2\theta & \sin^2\theta & 2\sin\theta\cos\theta \\ \sin^2\theta & \cos^2\theta & -2\cos\theta\sin\theta \\ -\sin\theta\cos\theta & \sin\theta\cos\theta & \cos^2\theta - \sin^2\theta \end{bmatrix}$$

and θ is defined as shown in Fig. 4.

Equations (21) and (22) enable the evaluation of eqns (12) and (13) by identification of the generalized stress–strain relationship

$$\{M_{xy}\} = [\lambda]^T[D'_{\alpha\beta} + D'_{s0} + D'_{0\beta}][\lambda]\{w_{,xy}\}. \tag{23}$$

To demonstrate the utilization of this general expression we present the results (in Newton, millimetre units) obtained for two perspex ($E = 3774$ N mm^{-2}, $\nu = 0.35$) plates using different methods.

Figures 7 and 8 show a plate ABCD, of symmetrical trapezoidal shape in plan, subject to a unit central point load. This problem is suitable for initial consideration due to the regular geometry of the plate, and the fact that the loading and boundary conditions are capable of being simulated with acceptable accuracy in the laboratory. Furthermore, although the twisting moments exhibit theoretical singular behaviour at the corners[10], the contributions of these singularities to the solution have been minimized by considering loading which generates a small amount of strain energy in these regions, and the theoretical solutions presented assume a single valued solution for the corner twisting moments.

The Rayleigh–Ritz results presented in Fig. 9 have been obtained using a solution process[11] based on eqn (10) with the constraint that $\delta\sigma_{kl} = 0$. Since a straightforward

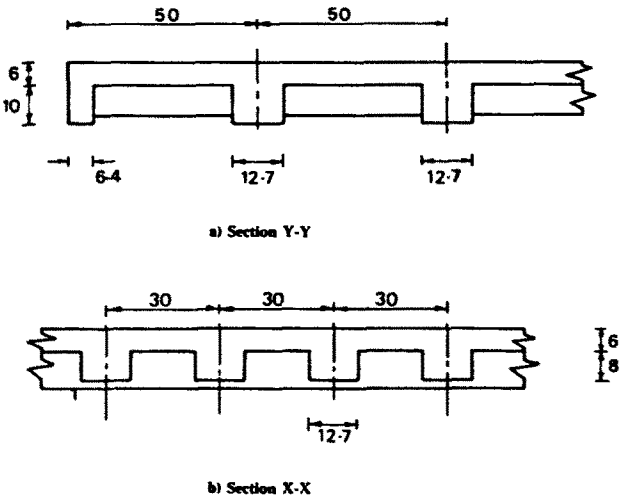

Fig. 8. Details of the stiffener dimensions for the plate illustrated in Fig. 7. All dimensions in mm.

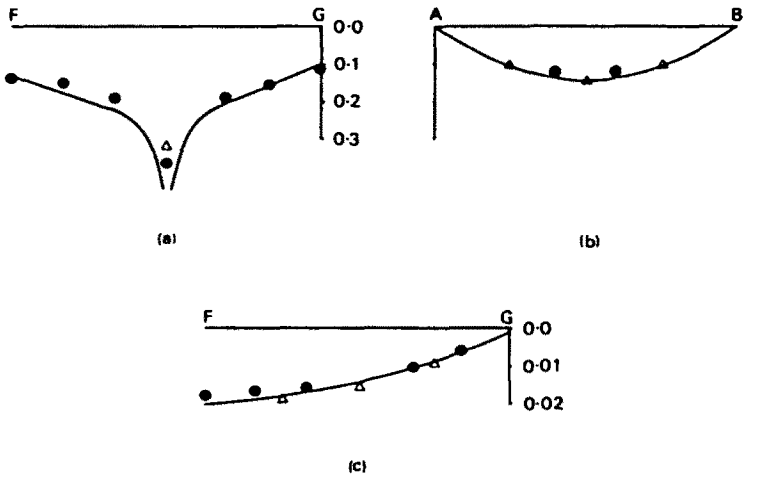

Fig. 9. Results obtained for the problem delineated in Figs 7 and 8. All values are in Newton millimetre units: (a) M_x on F–G; (b) M_x on A–B; (c) deflection on F–G. ——, Rayleigh–Ritz; ●, finite element; △, experimental result.

Rayleigh–Ritz approximation results in all defined field variable derivatives being explicitly prescribed continuous, the remedial action specified in Ref. [11] has been implemented to simulate the anticipated singularity in bending moments under the point load. The comparative finite element results have been obtained using a solution based on Reissner's form of eqn (11) (i.e. requiring the inverse of eqn (23)) which awards piecewise continuity to the bending moments, a finite weighting towards continuity of $M_{x,x}$ and $M_{y,y}$ but not $M_{x,y}$ and $M_{y,x}$ and independent linear and quadratic approximations to the moments and displacements within each element, respectively. The process is therefore able to interpret this problem as the limiting case of a continuous one in a manner very similar to the classical analysis provided a sufficiently fine mesh is used, and no specific allowance for the singular behaviour of M_x and M_y under the point load has been made. Both sets of theoretical results agree with those obtained experimentally to within the error bounds on the latter.

The plate WXYZ illustrated in Figs 10 and 11 tests the theory under significantly different (and more generalized) conditions of geometry and loading, and has the additional advantage that there is no singular behaviour of the field variables. The Rayleigh–Ritz results presented in Fig. 12 were obtained using Simpson's rule with 11 integrating points in each direction, and with the generalized stress–strain relationship of eqn (23) re-evaluated at each integration point. The finite element results were obtained using a regular 8×6 mesh of bisected quadrilaterals with eqn (23) assumed constant within each element and

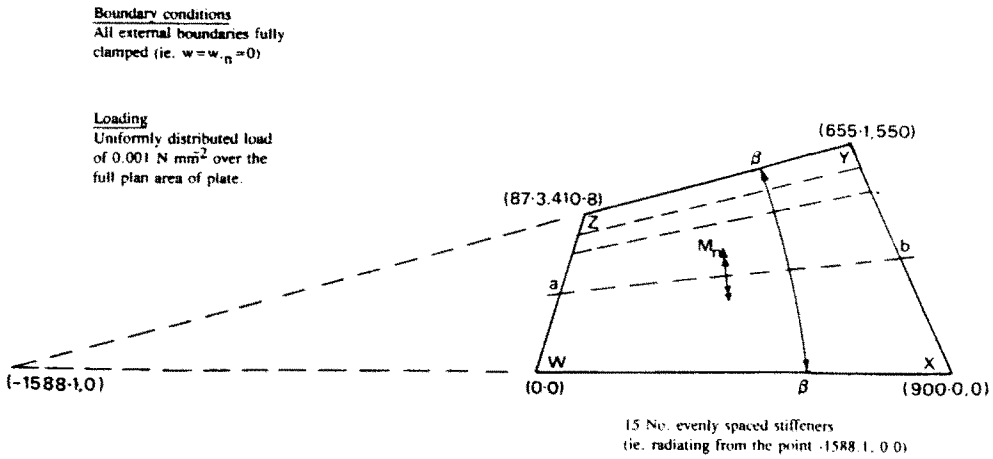

Fig. 10. Plan dimensions and boundary conditions of the plate WXYZ considered in Section 3.

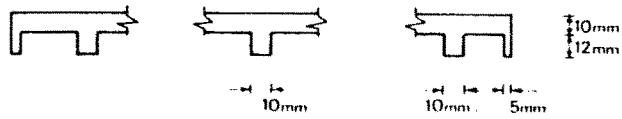

Fig. 11. Section β β through the plate illustrated in Fig. 10.

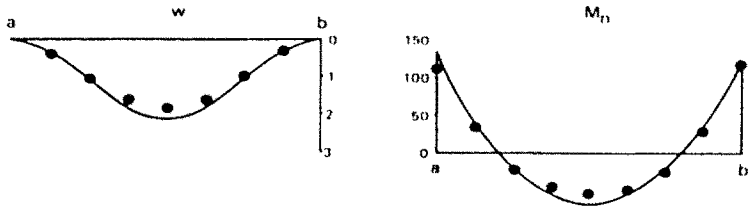

Fig. 12. Results obtained for the problem illustrated in Figs 10 and 11. All values are in Newton millimetre units: (a) deflection on A B; (b) M_n on A B. , Rayleigh Ritz; ●, finite element.

evaluated at the element centroids. These results demonstrate the numerical stability of the smoothing process on a typical stiffening pattern of practical significance covered by the generalized theory; no experimental results are available for this problem.

In view of the complexity of these problems, and the relatively weak weighted averages sought for the displacements through Reissner's principle[17] these results demonstrate the stability of the numerical process advocated here for the implementation of eqn (23) subject to the limitations obtained in Section 2.

4. AMENDED THEORY TO ALLOW FOR THE EFFECT OF THE STRAINS DUE TO POISSON'S RATIO ON THE POSITION OF THE NEUTRAL AXIS

In the previous analysis the neutral axes were located on the assumption that the bending stresses in the directions parallel to the stiffeners were independent. Simultaneously the bending moments were calculated including the effects of ν in the plate, thus destroying to an undetermined extent equilibrium in the plane of the plate. In the present analysis the neutral axes are defined as those of zero total strain in the α- and β-directions, and allowed to locate themselves so that equilibrium is restored. We shall continue to ignore the effect of ν in the stiffeners on the calculations, but note that the results demonstrate this is not important.

On the above basis it is possible to proceed assuming that all the information given in Figs 5 and 6 still pertains, but allow the neutral axes to locate themselves so that (if possible) a state of pure bending is obtained. In the α-direction, assuming the neutral axis (NA) occurs in the stiffener

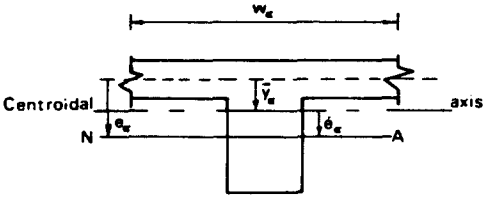

Fig. 13. Section β–β over a length equivalent to the local stiffener spacing: neutral and centroidal axes not necessarily coincident.

$$w_x \int_{-t/2}^{t/2} \sigma_x^p \, dz + b_x \int_{-(t/2+d_x)}^{-e_x} \sigma_x^s \, dz + b_x \int_{-e_x}^{-t/2} \sigma_x^s \, dz = 0. \tag{24}$$

Since the essential argument of this section is unaffected qualitatively by the degree of material orthotropy, it is convenient (for the purposes of clarity) to consider only isotropic behaviour with

$$E_{xx} = E_{\beta\beta} = E; \quad \nu_{x\beta} = \nu_{\beta x} = \nu \tag{25}$$

substituting eqns (19a), (15), and (25) into eqn (24), carrying out the appropriate integration, making the approximation that $(1-\nu^2) = 1$, and rearranging yields

$$e_x = \bar{y}_x - \nu\rho e_\beta \frac{A_x^p}{A_x} \tag{26}$$

(the same result is obtained if NA is assumed to occur in the plate) where A_x is the area of the full section illustrated in Fig. 13, A_x^s the area of the stiffener illustrated in Fig. 13, A_x^p the area of the plate illustrated in Fig. 13, $\bar{y}_x$ the distance from the mid-depth of the plate to the centroid of the stiffened section and

$$\rho = w_{,\beta\beta}/w_{,xx}$$

summing the horizontal forces in the β-direction yields

$$e_\beta = \bar{y}_\beta - \frac{\nu}{\rho} e_x \frac{A_\beta^p}{A_\beta} \tag{27}$$

where the terminology used in eqn (27) follows from that used in eqn (26). Substituting eqn (27) into eqn (26) and ignoring terms in ν^2 yields

$$e_x = \bar{y}_x - \nu\rho \frac{A_x^p}{A_x} \frac{A_\beta^s}{A_\beta}$$

or, substituting

$$\begin{aligned} A_x &= A_x^p + A_x^s; \quad e_x' = e_x - \bar{y}_x \\ e_x' &= \nu\rho\bar{y}_\beta\left(1 - \frac{A_x^s}{A_x}\right) \end{aligned} \tag{28}$$

where e_x' is the distance from the centroid to NA as shown in Fig. 13. Clearly a similar expression can be obtained for e_β'. From eqn (28) we deduce the following.

(1) e_x', e_β' are totally dependent on ν, and thus if effects due to Poisson's ratio are considered negligible e_x', $e_\beta' = 0$; $e_x = \bar{y}_x$; $e_\beta = \bar{y}_\beta$.

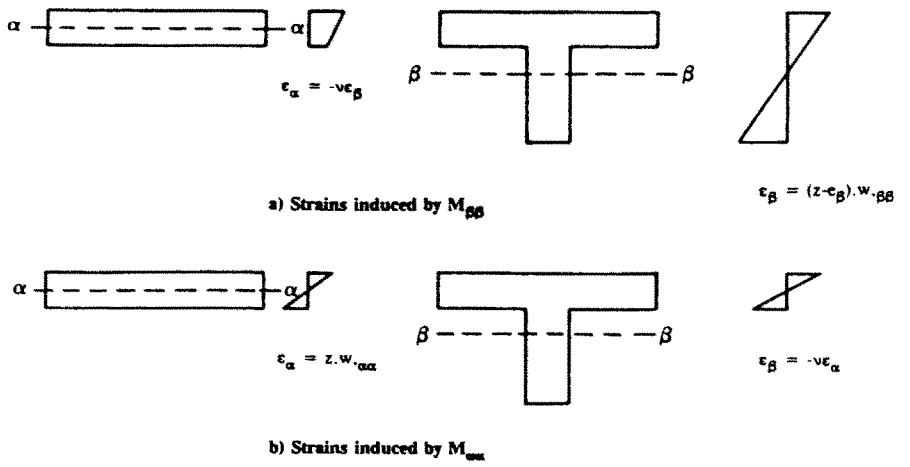

Fig. 14. Strains induced in a singly stiffened plate by application of (a) $M_{\beta\beta}$ and (b) $M_{\alpha\alpha}$ in turn.

(2) Equation (28) is a separable function of the displaced shape and plate dimensions, and each effect can therefore be discussed separately.

(3) The geometrical configuration which maximizes e'_α is large and closely spaced stiffeners in the β-direction, and no stiffeners in the α-direction. Indeed, Fig. 14 clearly shows that as $\bar{y}_\alpha$ decreases and $\bar{y}_\beta$ increases, a situation is always reached at which v can move NA totally outside the section for certain moment combinations. Consequently we surmise that in general, the application of transverse loading to a stiffened plate generates a condition of combined bending and axial stress of the type

$$\Omega = \tfrac{1}{2}M_{ij}w_{,ij} + \tfrac{1}{2}F_i\kappa_i \tag{29}$$

where both $i, j = \alpha, \beta$ in turn, F_i is the resultant axial force/unit width, and κ_i the generalized strain against which F_i does work.

(4) Cusens *et al.*[9] obtained very poor correlation between experimentally and theoretically determined estimates of the traditionally defined bending rigidities (cf. Section 3), about the weaker principal axis, for the situation illustrated in Fig. 14. The argument of (3) above shows that this is because the assumption of centroidal neutral axes is most in error under these conditions. However, this may not be a significant source of error in practical stiffened plate theory applications, as these generally fall into two categories.

(a) Predominantly singly spanning plates (in say the β-direction), with $M_{\alpha\alpha}$ generally significantly less than $M_{\beta\beta}$; for efficiency such plates are only stiffened about the β-β axis, thus

$$e'_\alpha > 0 \quad \text{but} \quad M_{\alpha\alpha} \doteq 0; \quad U_1 \doteq U_2.$$

(b) Doubly spanning plates, i.e. $M_{\alpha\alpha}$, $M_{\beta\beta}$ are of the same order; such plates are usually stiffened in both directions, thus

$$M_{\alpha\alpha}, M_{\beta\beta} > 0 \quad \text{but} \quad e'_\alpha, e'_\beta \doteq 0; \quad U_1 \doteq U_2$$

where U_1, U_2 are the theoretical strain energies in the stiffened plate with centroidal and fully consistent neutral axes, respectively.

Clearly, therefore, an upper bound on the effect of v on the location of the neutral axes can be obtained by re-analysing the doubly spanning, singly reinforced quadrilateral plate considered in Section 3, but this time using the constitutive equations defined by eqn (29).

Rather than attempt to formulate eqn (29) directly, it is more convenient to note that eqn (21) was effectively obtained by evaluating the work done per unit area of the plate by

Table 1. Illustrating the effect on the plate delineated in Figs 10 and 11 of substituting fully consistent for centroidal neutral axes

	Support conditions (restrained values)		Theoretical results at centre of plate (N, mm units)					
			Section 3			Section 4		
	WZ, XY	WX, ZY	w	$M_\alpha = M_x$	M_β	w	$M_\alpha = M_x$	M_β
1	w	none	20.4	660	24	20.1	652	30
2	$w; w_{,n}$	none	4.05	229	15	3.93	223	14
3	w	w	8.10	311	135	7.98	306	133
4	$w; w_{,n}$	w	3.41	206	61	3.31	201	62
5	$w; w_{,n}$	$w; w_{,n}$	2.18	134	59	1.93	114	47

the strains against the stresses for arbitrary e_x, e_β. The analyses of Section 3 were then carried out by putting

$$e_x = \bar{y}_\alpha; \quad e_\beta = \bar{y}_\beta.$$

It therefore follows that eqn (29) can be re-expressed in the form of eqn (21) with e_x, e_β derived through eqns (26) and (27). The solution to any given problem can then be sought by obtaining an initial solution assuming $\rho = 0$, re-evaluating ρ, and repeating the analysis until convergence is achieved.

Table 1 indicates the effect of using fully consistent neutral axes on the chosen plate using several different modes of support. In accordance with (a) and (b) above, using the support conditions for which this stiffening arrangement is efficient (analyses 1 and 2) the difference between the results obtained using the centroidal and consistent theories is minimal. Using the boundary restraints considered in analyses 4 and 5, errors of 3 and 11.5%, respectively, are obtained from the centroidal theory.

These results show that provided a plate is stiffened reasonably efficiently, negligible error will be induced by assuming centroidal neutral axes.

All the analyses summarized in Table 1 converged within three iterations; however, the equations are unstable when $\rho \simeq 0$, and the above results were obtained by putting $w_{,\beta\beta} = 0$ if $\rho < 0.1$.

5. ALLOWANCE FOR THE WORK DONE IN THE STIFFENERS DUE TO POISSON'S RATIO

Consider a small element of a plate subject to the restrictions under consideration in this paper, and the dimensions of which are defined by the terminology of Figs 5 and 6. Figure 15 shows such an element subject to biaxial tension in the principal directions of orthotropy. Over the volume $b_x b_\beta d_m$ (where d_m is the lesser of d_x, d_β) the work done by the strains due to Poisson's ratio in the stiffeners is given by

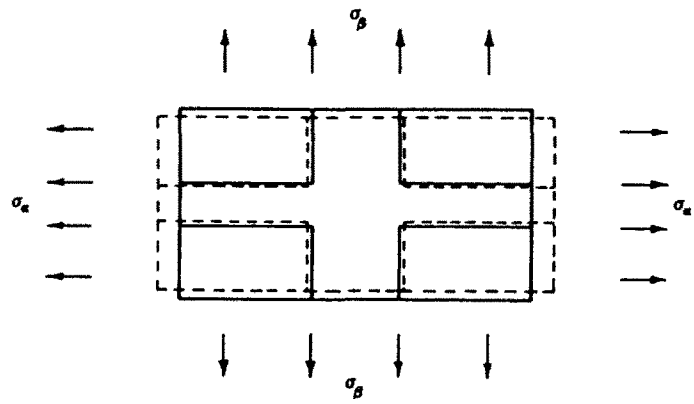

Fig. 15. Plan view of a typical element of a doubly stiffened plate subject to plane stress with $\sigma_x > \sigma_\beta$.

$$U^{\alpha\beta} = -\tfrac{1}{2}h_\alpha h_\beta d_m(\nu_{\alpha\beta}\varepsilon_\alpha\sigma_\beta + \nu_{\beta\alpha}\varepsilon_\beta\sigma_\alpha).$$

Thus for a plate in bending with ε_α, ε_β varying linearly with depth as illustrated in Figs 5 and 6, $U^{\alpha\beta}$ can be re-expressed in terms of the locally smoothed energy density, given by

$$\Omega^{\alpha\beta} = -\frac{h_\alpha h_\beta}{2f_\alpha f_\beta}\int_{(t/2-d_m)}^{(t/2)} (\nu_{\alpha\beta}\varepsilon_\alpha\sigma_\beta + \nu_{\beta\alpha}\varepsilon_\beta\sigma_\alpha)\,\mathrm{d}z. \tag{30}$$

In addition the direct stresses in the stiffeners are now related to the stiffener strains by eqns (15) over the volume of stiffener overlap. Thus Ω_i^α now becomes

$$\Omega_i^\alpha = \frac{E}{f_\alpha}\left(\frac{h_\alpha d_\alpha^2}{12} + h_\alpha d_\alpha h_\alpha^2\right)\left(\frac{h_\beta}{f_\beta(1-\nu^2)} + 1 - \frac{h_\beta}{f_\beta}\right) \tag{31}$$

and similarly for Ω_i^β.

The omission of these modifications to eqn (16) is acceptable if the volume of stiffener overlap is small in comparison with the total volume of the stiffened plate. However, as the slab thickens and stiffener spacings are decreased, so the stiffeners tend to dominate the behaviour, and significant errors in the strain energy density can be anticipated under these circumstances.

Since the effect of $\nu_{\alpha\beta}$ and $\nu_{\beta\alpha}$ on the movement on the neutral axes is minimized when the effect under the present discussion is a maximum (and vice versa), it is always permissible to allow for the latter by re-writing eqn (16) as

$$\Omega_i = \Omega_i^{\nu} + \Omega_i^{\alpha} + \Omega_i^{\beta} + \Omega_i^{\alpha\beta}. \tag{32}$$

Substituting eqns (15) and (19a) into eqn (30), carrying out the integration and substituting this result and eqn (31) into eqn (32) yields (cf. eqn (21))

$$\Omega_i = \tfrac{1}{2}\{w_{,\alpha\beta}\}[D'']\{w_{,\alpha\beta}\} \tag{33}$$

where $[D'] = [D]$ except that $D''[1,1]$, $D''[2,2]$ are modified according to eqn (31) and

$$D''[1,2] = D''[2,1] = D[1,2] + D''_{12}$$

with

$$D''_{12} = \frac{D_{12}h_\alpha h_\beta}{f_\alpha f_\beta}d_m\left[e_\alpha e_\beta - \frac{t}{2}(e_\alpha + e_\beta) + \frac{t^2}{4}\right]\frac{d_m^2}{2}[t-(e_\alpha+e_\beta)] + \frac{d_m^3}{3}.$$

Figure 16 shows the central displacements obtained defining the strain energy density by both eqns (21) and (33) for a simply supported square perspex plate (side length, 1000 mm; thickness, 5 mm; loading, 0.01 N mm^{-2}) stiffened by a regular grillage of beams 20 mm deep, 50 mm spacing, and widths varying from 10 to 50 mm. Also considered is a 25 mm thick unstiffened perspex plate of identical plan dimensions and subject to the same loading. The result so obtained is slightly smaller than by using eqn (33) to define the 5 mm plate with 50 mm wide stiffeners at 50 mm spacings. This is because the torsional stiffness of the latter is reduced by the 50 mm square grillage of 20 mm deep cuts. However, all other terms in the moment–curvature relationships are identical for both plates.

Equations (21) assume that the strains due to ν in the stiffeners occur without generating any stresses. For the plate and stiffener configurations considered in Fig. 16 this leads to results between 6 and 19% overflexible; similar discrepancies are obtained for the stresses. For practical applications it would appear therefore, that the use of eqns (33) in place of eqns (21) can eliminate significant errors without penalty.

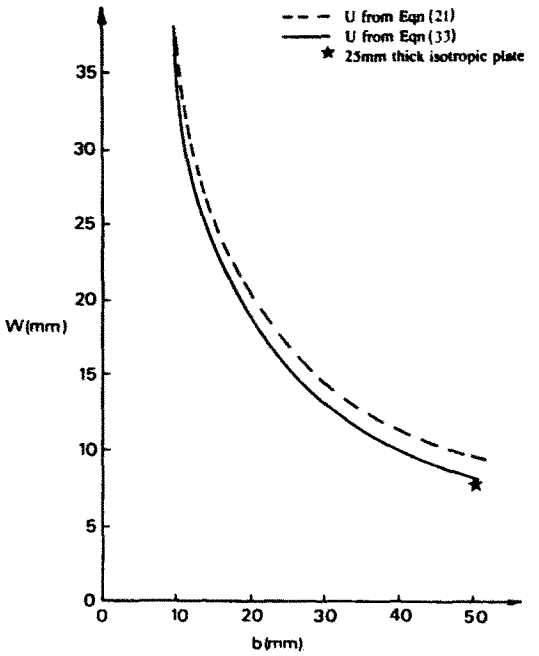

Fig. 16. Typical results obtained for the example problem considered in Section 5.

6. CONCLUSIONS

(1) The generalized conditions under which a 2-D analysis for thin (i.e. plan dimensions large in comparison to the cross-sectional ones) stiffened plates can be formulated are as obtained in Sections 1 and 2.

(2) A simple analysis assuming centroidal neutral axes resulting in an easily utilized set of generalized constitutive equations has been presented in Sections 3 and 5 for a class of stiffened plates which includes the vast majority of practical applications of stiffened plate theory.

The analysis can be reworked to include effects (c) (f) identified in Section 1 using established theory should they be considered significant in a given application. It was similarly considered that the conditions under which effects (h) are significant do not pertain.

If the stiffeners are widely spaced shear lag can be allowed for by assuming the shear strains are negligible and forming the energy in the system in terms of an additional parameter which enables the depth of the neutral axis to vary in such a manner that the shear lag equations[18, 19] are satisfied. If the stiffeners are of such a depth that the stiffened plate becomes moderately thick, the transverse shear stresses in the stiffeners can be simulated using an additional parameter which allows the stiffener cross-sections to rotate with respect to one another[2, 15].

(3) The assumption of centroidal neutral axes has, in Section 4, been shown to be sufficiently accurate under arbitrary conditions for engineering purposes; it has also been shown that for efficient stiffening patterns, the error so induced is negligible. However, the stresses generated in the stiffeners due to Poisson's ratio, which are also normally ignored, may be significant. In Section 5 it has been shown how these stresses can readily be taken into account.

REFERENCES

1. S. P. Timoshenko and S. Woinowsky-Kreiger, *Theory of Plates and Shells*, 2nd Edn. McGraw-Hill, New York (1970).
2. B. M. Irons and S. Ahmad, *Techniques of Finite Elements*. Ellis Horwood, Chichester (1980).
3. A. E. H. Love, *A Treatise on the Mathematical Theory of Elasticity*. Cambridge University Press, London (1927).
4. J. E. Ashton and J. M. Whitney, *Theory of Laminated Plates*. Technomic, Stamford (1970).

5. M. S. Troitsky, *Stiffened Plates—Bending, Stability and Vibrations*. Elsevier, New York (1976).
6. V. Z. Vlasov, *Thin Walled Elastic Beams*. Israeli Program for Scientific Translations, Jerusalem (1961).
7. R. Dabrowski, *Curved Thin Walled Girders* (Translated from German by C. B. Amerongen). Cement and Concrete Association (1978).
8. V. Kristek, Tapered box girders of deformable cross section. *A.S.C.E. Proc.* **96**(ST8), 1761–1793 (1970).
9. A. R. Cusens, M. A. Zeidan and R. P. Pama, Elastic rigidities of ribbed plates. *Bldg Sci.* **7**, 23–32 (1972).
10. L. S. D. Morley, *Skew Plates and Structures*. Pergamon Press, Oxford (1963).
11. J. C. Boot and D. B. Moore, An efficient analysis for thin plates of general quadrilateral shape subject to bending stresses. *Comput. Meth. Appl. Mech. Engng* **43**, 57–79 (1984).
12. S. P. Timoshenko and J. N. Goodier, *Theory of Elasticity*. McGraw-Hill, New York (1970).
13. K. Washizu, *Variational Methods in Elasticity and Plasticity*, 3rd Edn. Pergamon Press, Oxford (1982).
14. B. F. de Veubeke, Displacement and equilibrium models. In *Stress Analysis* (Edited by O. C. Zienkiewicz and G. S. Holister). Wiley, London (1965).
15. D. R. J. Owen and E. Hinton, *Finite Elements in Plasticity: Theory and Practice*. Pineridge Press, Swansea (1980).
16. I. S. Sokolnikoff, *Tensor Analysis: Theory and Applications to Geometry and Mechanics of Continua*. Wiley, New York (1964).
17. L. R. Herrman, A bending analysis for plates. *Proc. 1st Conf. on Matrix Methods in Structural Mechanics*, Wright-Patterson Airforce Base, AFFDL-TR-66-80, pp. 577–604 (1965).
18. M. Holmes, Uniform load on a slab or plate stiffened by beams. *Struct. Engr* **38**, 196–199 (1960).
19. A. O. Adekola, The dependence of shear lag on partial interaction in composite beams. *Int. J. Solids Structures* **10**, 389–400 (1974).